Article

Noise and Low-Level Dynamics Can Coordinate Multicomponent Bet Hedging Mechanisms

Javier Garcia-Bernardo[1] and Mary J. Dunlop[2,*]
[1]Department of Computer Science and [2]School of Engineering, University of Vermont, Burlington, Vermont

ABSTRACT To counter future uncertainty, cells can stochastically express stress response mechanisms to diversify their population and hedge against stress. This approach allows a small subset of the population to survive without the prohibitive cost of constantly expressing resistance machinery at the population level. However, expression of multiple genes in concert is often needed to ensure survival, requiring coordination of infrequent events across many downstream targets. This raises the question of how cells orchestrate the timing of multiple rare events without adding cost. To investigate this, we used a stochastic model to study regulation of downstream target genes by a transcription factor. We compared several upstream regulator profiles, including constant expression, pulsatile dynamics, and noisy expression. We found that pulsatile dynamics and noise are sufficient to coordinate expression of multiple downstream genes. Notably, this is true even when fluctuations in the upstream regulator are far below the dissociation constants of the regulated genes, as with infrequently activated genes. As an example, we simulated the dynamics of the multiple antibiotic resistance activator (MarA) and 40 diverse downstream genes it regulates, determining that low-level dynamics in MarA are sufficient to coordinate expression of resistance mechanisms. We also demonstrated that noise can play a similar coordinating role. Importantly, we found that these benefits are present without a corresponding increase in the population-level cost. Therefore, our model suggests that low-level dynamics or noise in a transcription factor can coordinate expression of multiple stress response mechanisms by engaging them simultaneously without adding to the overall cost.

INTRODUCTION

Cells can use stochastic gene expression (noise) and dynamics to diversify isogenic populations to hedge against stress (1). For example, in bacterial persistence, a small fraction of cells stochastically enters a dormant, drug-resistant state, allowing the population to insure against the sudden appearance of an antibiotic (2,3). An excitable gene circuit in *Bacillus subtilis* drives the temporary transition to competence under nutrient limitation (4,5). These are infrequent events: <1% of *Pseudomonas aeruginosa*, *Staphylococcus aureus*, and *Escherichia coli* cells are in the persistence state, and 3% of *B. subtilis* cells initiate competence under nutrient limitation (4–6). However, stress response mechanisms often require expression of many genes simultaneously, and single regulators may control many downstream targets. These observations raise the question of how multiple rare events are coordinated. A key principle of bet hedging is that the cost to the overall population is low, because only a small subset of cells initiates a response. We extended this idea by asking whether coordinated expression of downstream genes could further mitigate overall cost.

Single-cell resolution measurements have revealed that cellular processes involved in stress response and environmental change have high levels of phenotypic variability. For example, systematic noise measurements across the *Saccharomyces cerevisiae* proteome have demonstrated that noise levels are high for proteins involved in stress response, amino acid synthesis, and heat shock (7). TATA-box-containing genes associated with stress response in *S. cerevisiae* exhibit fluctuations that protect against future environmental changes (8). Variability can come from noise sources that are intrinsic or extrinsic, where intrinsic noise is unique to individual genes and variability is produced by random events in transcription, translation, and degradation. Extrinsic noise is produced by variability in processes that affect many genes in the same way; for instance, differences in growth or numbers of ribosomes in a cell can produce correlated expression of many genes (9–12). Diversity can also be driven by dynamic changes in gene expression as a result of the regulatory architecture. For instance, regulatory proteins can exhibit repetitive pulses in expression even in the absence of external inputs that drive this behavior (13,14). Examples of pulsing include the yeast regulator Msn2 under glucose, osmotic, and oxidative stress (15,16); Crz1 in response to calcium stress (17); and KatG in *Mycobacterium* to control persistence (18). Specific networks, such as coherent feed-forward loops, have been shown to increase population heterogeneity, enhancing drug resistance (19). Phenotypic diversity of stress-response mechanisms, derived from stochastic gene expression or other

Submitted August 12, 2014, and accepted for publication November 10, 2014.

*Correspondence: mjdunlop@uvm.edu

Editor: Reka Albert.

0006-3495/15/01/0184/10 $2.00

http://dx.doi.org/10.1016/j.bpj.2014.11.048

dynamics, plays an important role in protecting against future uncertainty.

Interestingly, many stress response mechanisms are members of single-input or multi-input modules, where one or a few regulatory proteins control the expression of many downstream genes (20). This regulatory motif is overrepresented in genetic networks that respond to exogenous conditions such as diauxic shift and DNA damage (21). In response to stress, Msn2 from *S. cerevisiae* regulates hundreds of target genes (15). Crz1 exhibits pulses that activate >40 genes (17). The alternative sigma factor σ^B in *B. subtilis* exhibits noise-driven pulses, regulating >100 genes (22). The multiple antibiotic resistance activator MarA in *E. coli* controls >40 downstream genes involved in resistance to antibiotics (23,24). Therefore, understanding how noise or dynamics in an upstream regulator influences expression of diverse downstream genes is of great interest in understanding stress response. An upstream regulator could potentially achieve the concentration necessary to activate the simultaneous expression of multiple downstream genes. However, achieving infrequent coordination in a small subset of the total population would require complex regulation or long-term memory. The alternative strategy presented here is to rely on low-level fluctuations in the activator to coordinate multiple rare events.

Whether a signal is propagated depends upon whether the downstream promoter can decode the variability in the transcription factor, as determined by the promoter and the properties of the signal (15,25–28). If the dynamics of the downstream promoter are fast, that is, the binding and unbinding rates are faster than degradation, cell division, and changes in the upstream input, then the output will follow the input (25). If they are slow, then most of the input dynamics will be filtered (16). For example, input pulses that are high in amplitude or duration will activate the promoter (16), but small pulses and noise that do not meet these requirements will rarely activate downstream promoters. Although activation is infrequent, the downstream genes will still be activated a small fraction of the time due to the stochastic nature of gene expression; these rare events produce long tails in the mRNA and protein distributions (29–31).

There is a cost associated with the expression of stress-response genes. In general, cells allocate their resources to optimize growth, but the expression of genes not immediately related to growth can provide a potential benefit if the environment changes. This cost-benefit relationship has been observed in vivo: for lactose intake, populations of *E. coli* are able to grow fastest in the presence of lactose if the *lac* operon is expressed moderately, but not if expression is high (32). For antibiotic resistance, cells are able to grow in higher concentrations of antibiotic if the *mar* operon is moderately induced (33,34). Therefore, there is a tradeoff between the burden imposed by the expression of these genes and the benefits they can provide in an uncertain environment.

To understand how noise and dynamics in a stress response regulator are propagated to downstream target genes, we performed stochastic simulations using three types of inputs: constant expression, pulsatile dynamics, and intrinsic/extrinsic noise. The regulators control the expression of several downstream genes, creating a single-input module similar to those observed in natural networks. We found that downstream genes regulated by all types of inputs have noisy expression profiles; however, fluctuating inputs (due to pulsatile dynamics or intrinsic/extrinsic noise) can coordinate the temporal pattern of downstream gene expression. This effect becomes pronounced when there are several downstream genes, because the probability of multiple genes being coordinated is higher when a dynamic input can orchestrate the response. The fidelity with which the input is propagated to the downstream genes depends upon the characteristics of the downstream promoter and the input signal. Notably, even low-level fluctuations in an upstream regulator can serve to hedge against stressors without adding to the overall cost. Coordination of downstream genes may allow cells to hedge against future uncertainty in the environment without an excessive burden to the population.

MATERIALS AND METHODS

Stochastic model

All downstream genes in all simulations are subject to intrinsic noise. To simulate this, we used a stochastic model based on the processes described below, for which the reaction rates are given in Table S1 in the Supporting Material and shown in Fig. S1. Exact stochastic simulations were conducted using the Gillespie algorithm (35).

Binding and unbinding of the regulator to the promoter of the downstream gene are modeled by

$$P + A \xrightarrow[K_{ON}]{} P'$$

$$P' \xrightarrow[K_{OFF}]{} P + A,$$

where P represents the promoter in the unbound state, A is a transcription factor, and P' is the promoter in the bound state.

Transcription and translation are modeled using

$$P \xrightarrow[\alpha]{} P + M$$

$$P' \xrightarrow[\alpha']{} P' + M$$

$$M \xrightarrow[\beta]{} M + D,$$

where M is the mRNA for the downstream gene and D is the protein encoded by the downstream gene. Presence of the transcription factor increases the transcription rate ($\alpha' > \alpha$). The translation rate, β, includes both translation and folding events.

mRNA and protein degradation are modeled by

$$M \xrightarrow[\lambda_M]{} \varnothing$$

$$D \xrightarrow[\lambda_D]{} \varnothing,$$

where the rates λ_M and λ_D model mRNA and protein degradation and dilution due to cell growth.

We considered constant and pulsing inputs for the transcription factor profiles. For the constant case, the activator level is set to 250 molecules for all time. To define the activator levels, the pulsing input case uses the function

$$A = \begin{cases} 500\left(1+\sin\left(\frac{t}{6\pi}-\frac{\pi}{2}\right)\right), & 0<t\leq 120 \\ 0, & 120<t<240 \end{cases}.$$

The signal is repeated every 240 min, creating periodic pulses of the regulator. The mean of the pulsing signal is 250 molecules, identical to the mean of the constant activator. We used an arbitrary periodic waveform represented by a sine wave followed by a period with no activator, so that signal properties including amplitude, pulse duration, and frequency could be adjusted explicitly.

Cross correlation

The cross correlation measures the correlation between two time series, $f(t)$ and $g(t)$, when a lag, τ, is applied to one of the two signals. We used the unbiased estimate of the cross correlation:

$$R_{f,g}(\tau) = \begin{cases} \frac{1}{N-|\tau|}\sum_{t=0}^{N-|\tau|-1} f(t+\tau)g(t), & \tau\geq 0 \\ R_{g,f}(-\tau), & \tau<0 \end{cases}.$$

Here, $f(t)$ and $g(t)$ are the time series for the transcriptional regulator and a downstream protein. Both signals are mean subtracted and normalized by dividing by the standard deviation. N is the number of time points.

Amplitude response plots

For three different dissociation constant (K_D) values (100, 1000, and 10,000 molecules), we varied the amplitude of the pulses from 10^{-2} K_D to 10^2 K_D, and ran a simulation keeping all other parameters constant. The resulting time series for the protein levels of the activator and downstream genes were used to calculate the maximum cross correlation.

Cost functions

We developed functions describing the cost and benefit of expressing a downstream gene. The cost term has two parts: a term c_1 that quantifies the burden of expressing proteins that are not needed for growth under baseline, nonstressed conditions, and a second term, c_2, which quantifies how cells are impacted in an environment with a stressor present. The total cost is assumed to be Bliss-independent (36) and is given by

$$c(D,S) = c_1 + c_2 - c_1 \times c_2,$$

where the cost is a function of the downstream protein levels, D, and the stressor, S.

The burden of protein expression is modeled as in Dekel and Alon (32):

$$c_1(D) = \frac{n_0 D}{1-\frac{D}{M}},$$

where M is the maximal capacity for nonessential proteins, D is the concentration of the downstream protein, and n_0 is a normalization constant.

The impact of a stressor is modeled as in studies by Wood and Cluzel (33) and Greco et al. (37):

$$c_2\left(S_{\text{eff}}\right) = \frac{S_{\text{eff}}^n}{k^n + S_{\text{eff}}^n},$$

where S_{eff} is the effective concentration of the stressor, k is the half-inhibition constant, and n is the Hill coefficient.

Following the formulation from Wood and Cluzel (33), the benefit is measured as a decrease in c_2. By decreasing the intracellular concentration of toxic compound, the relation between the extracellular concentration of the stressor, S, and the effective concentration, S_{eff}, is

$$S_{\text{eff}} = \frac{S}{1+B},$$

where B is the benefit of expressing the stress response machinery, given by

$$B(D) = \frac{b_{\max} D}{k_b + D}.$$

Here, $b_{\max}$ is the maximum benefit of expressing the machinery and k_b is the concentration of protein that gives the half-maximal response.

We used the following parameter values in the cost and benefit equations: $M = 15{,}000$ molecules, $n_0 = 1 \times 10^{-5}$, $k = 1$ mM, $n = 2$, $b_{\max} = 10$, and $k_b = 15{,}000$ molecules. M and n_0 were set such that $c_1(D)$ falls between 0 and 1. k sets the maximum concentration of stressor that the cells can survive when no resistance mechanisms are expressed, and n determines the steepness of $c_2(S_{\text{eff}})$, whereas $b_{\max}$ and k_b together set the maximum concentration that cells can survive when the resistance mechanisms are present. The results are not specific to the values used. We also tested another cost function, which depends linearly on the levels of D, $c_1(D) = D/M$ (Fig. S2), and observed similar benefits with coordination.

Maximum survivable concentration of stressor and cost without stressor

To quantify the maximum concentration of stressor that a population of cells can survive, we calculated the cost for each cell with the stressor (recall that the benefit of expressing resistance genes reduces the cost) and determined which cells survived. To determine survival, we imposed an arbitrary threshold of 0.95. Cells that exceed this threshold are dead and those with costs below it survive. We increased the concentration of the stressor until only 0.1% of cells in a simulated population of 10^6 cells survived. We define the concentration at which this occurs as the maximum survivable concentration. Our findings are not sensitive to the exact threshold values selected.

We performed these calculations by simulating long time courses (10^7 min) to generate distributions of downstream protein levels. Using this distribution, we calculated the cost for each point in the distribution. We verified that distributions of downstream protein levels generated using this approach are equivalent to those generated by running many shorter simulations and extracting data associated with the final time point (see Supporting Materials and Methods and Fig. S3).

The cost of growing without a stressor was calculated as the average of the costs for each of 10^7 cells in the simulation.

Multiple antibiotic resistance operon in *E. coli*

We simulated expression of genes in the *mar* operon, as in Garcia-Bernardo and Dunlop (38), using the Gillespie algorithm to obtain values of MarA as a function of time. Experimental data is available for the K_D values of nine downstream genes (39). We simulated 40 downstream genes by including multiple instances of each of the known values. The specific K_D values, assuming a cell volume of 10^{-15} L, are 7,830 (4), 10,239 (4), 15,058 (8), 18,069 (20), and 24,092 (4) molecules, where the number of instances of each gene included is shown in parentheses.

Extrinsic and intrinsic noise in the activator

To model extrinsic noise, we allowed K_{ON} to vary with time (as in Shahrezaei et al. (40)) in the activator and downstream genes. We used an exact numerical solution of an Ornstein-Uhlenbeck process. Extrinsic noise was simulated using the method of Gillespie (41), with code from http://www.mathworks.se/matlabcentral/fileexchange/30184-exact-numerical-simulation-of-the-ornstein-uhlenbeck-process. The code generates a time series for a source of extrinsic noise $\varepsilon(t)$, with zero mean and standard deviation equal to

$$\sigma = \sqrt{c \times \frac{T}{2}}.$$

The relaxation time, T, was set to 40 min (42), and the diffusion constant, c, was set to 0.006 (low noise), 0.02 (medium noise), 0.05 (high noise), where the parameters used in Shahrezaei et al. (40) fall between our medium and high noise cases. Following methods of Shahrezaei et al. (40) and Fox et al. (43), we replaced the parameter K_{ON} with

$$K_{ON} \times \frac{e^{\epsilon(t)}}{\langle e^{\epsilon(t)} \rangle},$$

which generates a lognormal distribution, suitable to model fluctuations due to extrinsic noise (26,40,42).

We modeled intrinsic noise in the activator using the Gillespie algorithm (35). Reactions and rates are the same as those for the downstream genes given in Table S1, with the following modifications: $K_{OFF} = 0.1$ min^{-1}, $K_{ON} = 1$ (molecules min)$^{-1}$, $\alpha' = 1$ min^{-1}, $\lambda_M = 0.1$ min^{-1}, $\beta = 1$ min^{-1}, and $\lambda_D = 0.02$ min^{-1}.

Although mean activator expression is identical for the three noise levels, the mean of the downstream gene will depend upon the noise levels. To correct for this, we adjusted K_{ON} for the downstream genes, as indicated in Table S2.

Based on the method of Shahrezaei et al. (40), we handled time-dependent propensities, $a(t)$, in the Gillespie algorithm by approximating $\int_t^{t+\tau} a(t)dt$ with $a(t)\tau$. This approximating is valid when changes in $a(t)$ are slow compared with the reaction times (i.e., the difference between $a(t)$ and $a(t+\tau)$ is small), as is the case in this study.

Coordination of *n* downstream genes

To calculate the fraction of cells in a population with n downstream genes expressed in a coordinated fashion we ran simulations of n downstream genes for 10^7 minutes, each using the same activator profile as input. For each time point, we checked how many cells had all downstream genes coordinated simultaneously. To measure this, we set a threshold of 1000 molecules and counted the number of downstream genes that exceeded the threshold. The fraction of cells with coordination in n genes is determined by dividing the number of cells where all n downstream genes exceeded the threshold by the number of cells where this was not achieved. Our results are not sensitive to the exact threshold values selected.

RESULTS AND DISCUSSION

Input dynamics can coordinate rare events

To study how expression of multiple downstream genes is impacted by the dynamics of a single input, we developed a stochastic model in which the promoter of a downstream gene can be in one of two states (44–46). In the active promoter state, a transcriptional activator is bound, leading to elevated levels of transcription relative to the inactive state, where the activator is not bound. The model includes reactions for transcription, translation, and degradation of mRNA and proteins (Methods). Many transcriptional regulators are expressed at basal levels and activated in the presence of stress, such as heat, nutrient limitation, or other environmental factors. Under unstressed conditions, having a small subset of the population express these genes can act as an insurance policy against future uncertainty. Furthermore, transcription factors operate on diverse downstream genes with a range of dissociation constants (K_D). This includes transcription factors with K_D values well above the physiological levels of the activator (see examples in the literature (16,39,47,48)). This allows a single transcription factor to differentially activate each of its downstream target genes. Therefore, we focused on downstream target genes with promoters that have K_D values well above the mean of the input (Fig. 1). By doing this, we are looking at rare events, as would be expected in bet hedging.

Initially, we compared two alternative upstream regulator dynamics and their impact on the expression of downstream genes. In the first case, the activator is held constant. In the second case, we considered a transcription factor that exhibits pulsatile expression, with a pulse followed by a

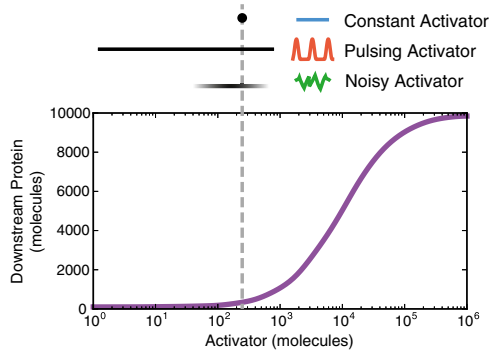

FIGURE 1 Input dynamics for a downstream gene. Activation curve for a downstream gene with a dissociation constant (K_D) of 10,000 molecules. The range of three activator dynamics is displayed above the figure: constant, pulsing, and intrinsic/extrinsic noise. In each case, the mean of the activator signal (*gray dashed line*) is identical. To see this figure in color, go online.

constant off state. We use the term pulsing here to describe time-varying signals, ranging from periodic oscillations to stochastic fluctuations in protein levels (13). For simplicity of analysis, we initially used a periodic input signal with uniform pulses followed by periods of low activator levels (Materials and Methods). However, as discussed later, our results do not require that the expression of the transcription factor be periodic or the pulse sizes uniform. We set the mean expression of the two transcription factors (constant and pulsing) to be identical to allow for a controlled comparison between the two types of input dynamics.

Even with a constant input, intrinsic noise due to stochastic events causes noise in expression of downstream genes (Fig. 2 *A*). Similar dynamics were observed in the pulsing case, but the transcription events are associated with the input pulse (Fig. 2 *B*). Because the fluctuations in the input are low compared with the K_D of the downstream gene, the transcription factor only intermittently turns on downstream gene expression and most variation is due to intrinsic noise. Although not every pulse in the input initiates expression of the output, when transcription is initiated, it is coordinated with the input pulse. When averaged over many downstream genes, fluctuations from the constant-input case average out, whereas fluctuations from the pulsed-input case follow the input (Fig. 2, *A* and *B*). Importantly, the distributions of downstream proteins are very similar for constant and pulsing inputs and have similar tails (Fig. 2 *C*), indicating that the frequency with which the downstream genes are in an elevated state of expression is similar for genes under both types of control. These results suggest that it is important to consider the timing of when genes are expressed and not just static expression data.

We next asked how propagation of input dynamics depends on the dissociation constant of the promoter for the downstream gene. We calculated cross correlations between the input signal and the downstream proteins. The cross correlation measures the similarity of two signals as a function of time (Materials and Methods). Because expression of the downstream gene follows the input pulse, there is a lag in the cross correlation, with the maximum cross correlation indicating how well the two signals are correlated after the signal is transmitted. As expected given the lack of input dynamics, there is no correlation between the input and downstream protein levels in the constant case, regardless of K_D (Fig. 2 *D*). In contrast, the pulsing input produces correlations between the input signal and the downstream protein. The highest correlations are from cases where the K_D is near or below the mean of the input, as expected, since it is easy to activate expression of downstream genes whose promoter has high affinity for the activator. As the K_D increases, the correlation goes down. Notably, the correlation persists for K_D values two orders of magnitude above the mean of the activator. Therefore, even infrequent activation events show correlation with the input signals, despite being far from the dynamic range of the downstream gene. This result is important because it suggests that even genes that appear

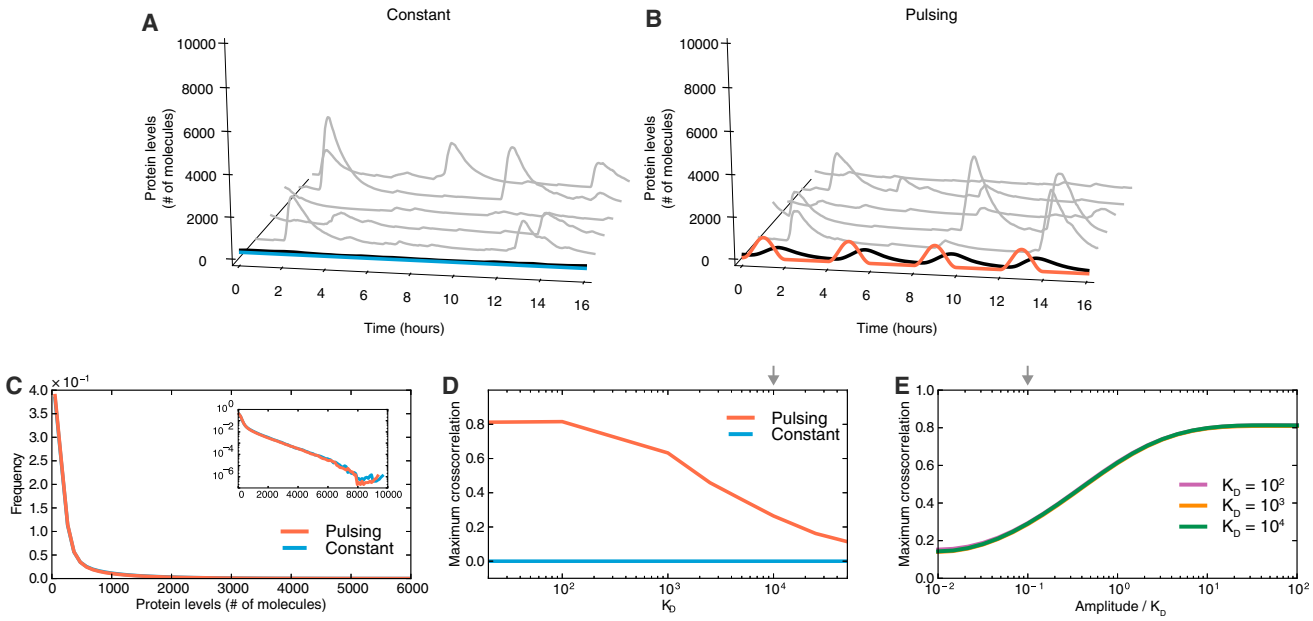

FIGURE 2 Pulsing-coordinates expression of downstream genes. (*A* and *B*) Downstream gene expression given a constant (*blue*) or pulsing (*red*) input. Protein levels for five representative downstream genes (*gray*) are shown, along with the mean of 1000 genes (*black*). (*C*) Histograms of downstream protein expression for constant and pulsing activator dynamics. (*Inset*) Same data as in the main figure, but on a semilogarithmic scale. (*D*) Maximum cross correlation between the activator signal and downstream protein as a function of K_D. The K_D used in the simulations shown in *A*–*C* is marked with an arrow. (*E*) Maximum cross correlation between a pulsing activator and three downstream genes with different dissociation constants as a function of the amplitude to the K_D ratio. The ratio used in the simulations in *A*–*C* is indicated with an arrow. To see this figure in color, go online.

not to be activated in population studies may be initiated rarely but in a coordinated fashion, providing an organized response, as might be necessary for bet hedging.

We also asked what impact the amplitude of the pulsing input has on the maximum cross correlation. When normalized by the K_D, the maximum cross-correlation curves are equivalent for all amplitudes (Fig. 2 *E*). Therefore, the important quantity is the ratio of the pulse amplitude to the K_D, with fluctuations well below the K_D still resulting in measurable levels of correlation between input and output signals. These results are consistent with those of previous studies showing that pulses in gene expression can be propagated: in Msn2 in yeast (15), NF-κB in mice (49,50), and the stress sigma factor σ^B in *B. subtilis* (22), pulses in the input are highly correlated with pulses in their respective downstream genes.

To test the generality of our results, we examined a system with fast promoter binding dynamics. In this case, transcription-factor binding and unbinding at the promoter is rapid, such that expression of the downstream gene is initiated more frequently, but the duration of each burst of expression is shorter (Supporting Materials and Methods). Again, we observed correlation between the pulsed input and the downstream output for K_D values well above the mean of the pulsed input (Fig. S4 *A*). We also asked whether our results were resistant to the inclusion of explicit cellular growth and partitioning and found that those processes have only minor contributions to the correlation observed between activator and downstream gene, as well as between two downstream genes (Supporting Materials and Methods and Fig. S5).

Coordination is achieved without added cost

We next asked what role the correlation between pulses in the input and initiation of expression of the downstream genes had on the regulation of multiple genes. As a model for a single input module, we simulated expression of 10 downstream genes, all regulated by a single transcription factor. We conducted numerical experiments with increasing concentrations of stressor, quantifying the maximum concentration of stressor that a population can survive (Materials and Methods). In addition, we calculated the population-level cost of expressing stress resistance genes using a cost function that we derived from previously published studies (Materials and Methods). When the input regulates a single downstream gene, both the maximum concentration of stressor that the population can survive and the population-level cost are similar for constant and pulsing inputs (Fig. 3 *A*). This result is expected, since the distribution of downstream proteins is equivalent for the two types of input (Fig. 2 *C*). However, when multiple genes are regulated together, populations with pulsing inputs are able to coordinate their response and survive higher concentrations of a toxic compound while maintaining equal costs (Fig. 3 *B*). Even modest benefits can provide a selective advantage, because they come with no added cost. Results for fast promoter binding dynamics (Fig. S4, *B* and *C*) and an alternative cost function (Fig. S2) are similar. Our results are consistent over a broad range of conditions, cost functions, and model parameters, indicating the generality of our findings. By coordinating downstream genes so that multiple stress-response mechanisms are engaged simultaneously, a pulsing input can achieve higher stress tolerance without added cost.

We note that the downstream genes modeled here all have high dissociation constants. This represents a conservative scenario; genes with lower K_D values or a mixture of downstream genes will exhibit greater benefits from coordination. We verified that downstream genes with higher affinity for the activator (lower K_D) achieve benefits from coordination (Fig. S6). In this case, the cost associated with input dynamics is lower due to the nonlinear nature of the activation curve. Therefore, input dynamics provide two benefits: frequently activated genes can enhance stress tolerance and also maintain a lower overall cost.

Nonperiodic pulsatile dynamics and extrinsic noise can coordinate downstream genes

Although we initially examined well-defined pulsatile signals to carefully control for pulse properties, we next asked whether our results could be generalized to other types of time-varying input. To test this, we used a model of the *E. coli* multiple antibiotic resistance activator (MarA) developed previously by our group (38). The multiple antibiotic resistance network is involved in protection against many stresses, including antibiotics, solvents, and other antimicrobial compounds (39,51). In this network, genes for the activator MarA and the repressor MarR are encoded in a single operon, which is regulated by both MarA and MarR, resulting in both positive and negative feedback controlling expression of the operon. Rapid increases in the level of MarA, followed by delayed inhibition by MarR may cause stochastic pulses in the expression of MarA (38). Once expressed, the regulator MarA activates over 40 genes with diverse K_D values, all of which exceed the mean concentration of the activator by at least an order of magnitude (39,52). We used this signal as an input to 40 representative downstream genes, selecting genes with a range of dissociation constants to match those measured in the literature (39) (Materials and Methods). We measured the maximum survivable concentration of an antibiotic stressor for a single gene and the suite of diverse downstream genes (Fig. 3, *C* and *D*). In each case, we compared the results to a model with a constant MarA input with a mean identical to that in the dynamic case. Consistent with our results using a well-defined pulse as an input, we found that stochastic pulses enable survival in higher concentrations of antibiotic stressors while maintaining similar or lower cost profiles.

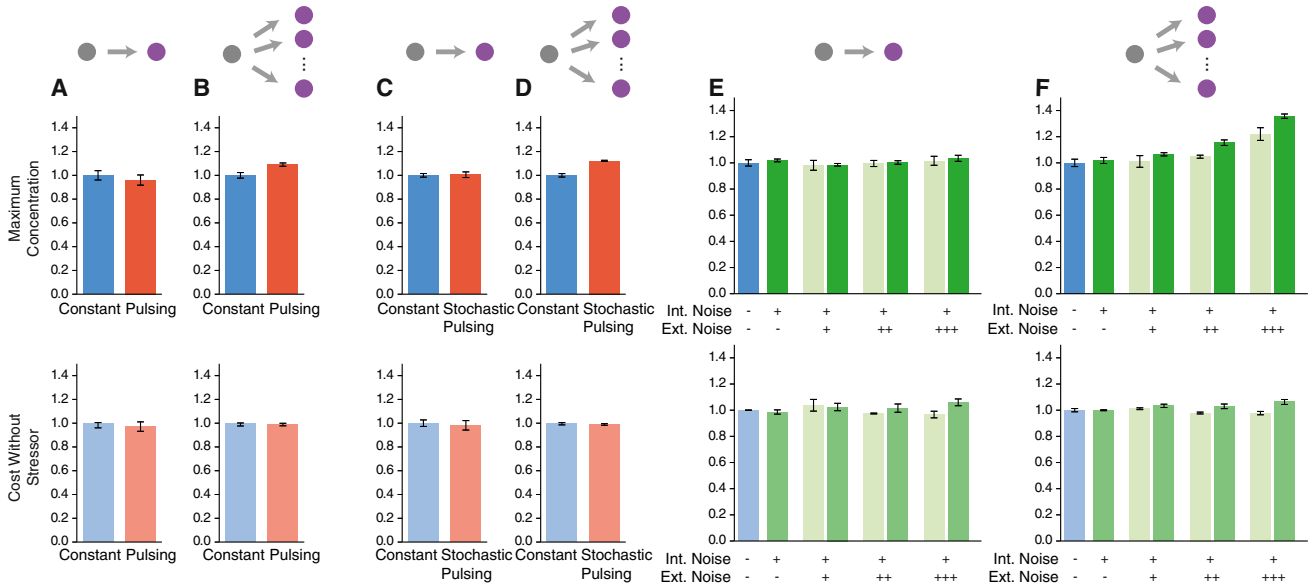

FIGURE 3 Coordination acts as a bet-hedging strategy with no added cost. (*A* and *B*) Maximum concentration of stressor that 0.1% of cells in a population can survive and the corresponding average cost of growing in the absence of stressor. Values were measured for constant and pulsing activator dynamics for one downstream gene (*A*) and 10 downstream genes (*B*), all with $K_D = 10{,}000$ molecules. (*C* and *D*) For the *mar* operon in *E. coli*, values were measured for constant and fluctuating MarA dynamics for one downstream gene with $K_D = 18{,}069$ molecules (*C*) and 40 downstream genes with experimentally derived dissociation constants (*D*) (see Materials and Methods). (*E* and *F*) Maximum survivable stressor and cost were measured for constant and fluctuating dynamics for different levels of noise in the activator and/or downstream genes for one downstream gene (*E*) and 10 downstream genes (*F*) with $K_D = 10{,}000$ molecules. Dark green bars show results with extrinsic and intrinsic noise in the activator and all downstream genes (cases with $\eta_{ext} = 0$, 0.11, 0.20, and 0.27 for the activator are shown). Light green bars show the contributions from extrinsic noise alone. For these simulations, there is no upstream activator, and downstream genes all have unique intrinsic noise and identical extrinsic noise signals. In all plots, values from the fluctuating dynamics are normalized to the constant input case. Error bars show standard deviations over three simulations. To see this figure in color, go online.

These results suggest that our findings on pulsatile inputs can be generalized to other dynamic regulators that control many downstream genes.

Noise in an upstream regulator has the potential to play a coordinating role if it is propagated to or affects all downstream genes in the same way (26,27). We considered both intrinsic and extrinsic noise sources in the input, where all genes are affected by unique intrinsic noise and identical extrinsic noise signals (12,26). We modeled extrinsic noise using an Ornstein-Uhlenbeck process and introduced fluctuations in the transcription-factor binding rate for all genes simultaneously, as in Shahrezaei et al. (40) (Materials and Methods). We calculated the maximum survivable stressor and the associated cost under increasing extrinsic noise. For regulation of a single downstream gene, adding extrinsic noise does not increase the maximum survivable stressor concentration (Fig. 3 *E*). However, when extrinsic noise affects multiple downstream genes, the coordination effect is visible (Fig. 3 *F*). In all cases, the cost is not highly impacted, so these gains are effectively free. Since extrinsic noise affects all genes simultaneously, it serves as a coordinating factor, which is combined with the noise dynamics introduced by the common upstream regulator; both contribute to the coordination of downstream genes (Fig. 3 *F*). This finding is consistent with experimental data on coordination in the yeast stress-responsive transcription factors Msn2/4 (11). Fluctuations in an upstream regulator provide a tunable mechanism to control coordinated stress response, and noise sources extrinsic to the stress-response pathway can add to this effect.

The timescale over which downstream genes remain coordinated is also important, as it determines whether beneficial effects will be passed on to daughter cells (53). To test this, we calculated the cross correlation between expression of downstream genes and found positive correlations that persisted well beyond the length of the cell cycle (Fig. S7). This timescale is sufficient for the activation of other resistance mechanisms that rely on sensing of the environment. Thus, input fluctuations can produce correlated expression of downstream genes over a timescale sufficient to produce resistant populations.

Dynamic inputs always outperform constant inputs in achieving coordination

We next asked what impact the number of stress response genes has on survival in the context of bet hedging. In cases where stress-response mechanisms are composed of several genes that work together to protect the cell, if these mechanisms are initiated by random events, then as the number of resistance genes goes up, the chances that they are coordinated at any given time goes down. We measured the

fraction of cells in a fixed size population that exhibit coordinated expression of downstream genes given different types of input (Fig. 4). For a single downstream gene, constant, pulsing, and noisy inputs are equally good, because there is no coordinating effect, but as the number of downstream genes increases, the benefit of input dynamics becomes apparent. Dynamics in the input play a coordinating role when there are multiple downstream genes, leading to a larger fraction of the population that can survive the sudden appearance of a stressor. If the promoters for downstream genes have higher affinity for the activator (lower K_D), a pulse in the input will frequently activate expression, resulting in cells with many coordinated downstream genes (Fig. S6 *D*). Therefore, the results for the high-K_D case shown in Fig. 4 are a conservative example of the benefits of input dynamics. Our findings are further supported by a simple mathematical model of input dynamics (Supporting Material).

CONCLUSIONS

The analysis presented here reveals an important role for noise and dynamics in inputs that control several infrequently activated downstream targets. Initiating expression of suites of stress-response genes in response to environmental signals might be too slow to deal with sudden catastrophic events. Diversifying phenotypes within a population before the crisis strikes can help ensure survival of a subset of the population (54). Such an approach is advantageous when the appearance of a stressor is rare and expression of stress-response machinery is costly.

Here, we asked about the scenario where stress response requires the coordinated action of several genes expressed simultaneously in a small fraction of the population. Examples where multiple mechanisms work in concert are common. Using a stochastic computational model, we examined the single-input-module regulatory motif, where one transcription factor regulates several downstream targets. In all cases, intrinsic noise in expression of the downstream genes leads to diversity within the population. However, if the upstream regulator is dynamic, for example, due to pulsatile expression or noise, it can drive coordination of diverse downstream target genes. Importantly, we found that even minor fluctuations in a transcription factor that regulates several target genes are sufficient to orchestrate coordination within a small subset of the population. Even for K_D values two orders of magnitude above the mean of the input, there is a measurable correlation with the dynamic input. We found that the overall cost with dynamic inputs is the same as or lower than that with constant inputs, and the maximum survivable concentration of stressor is the same or higher. Therefore, the benefits of coordination are in effect free. Because our findings test for rare events, only a small number of cells need to achieve coordination.

In contrast to strategies where two subpopulations of cells exist, as with bacterial persistence, coordination can allow for a graded response within the population. Because the activation of downstream gene expression is stochastic, there will be a distribution of stress-response phenotypes within the population, as opposed to an all-or-none response. In the future, it will be interesting to contrast the conditions under which distinct subpopulations and distributions each perform well and to compare these effects to sensory responses without stochastic effects (55).

The coordination of multiple downstream genes represents an alternative view on bet hedging to counter future environmental uncertainty. When the mean of the input is well below the dissociation constant of downstream genes, these genes are activated rarely. Most changes in input are filtered, but dynamic inputs ensure that when a downstream gene does turn on, it does so at a time when other genes may also be on. Here, we considered rare events, but we note that when the mean of the input is close to the dissociation constant of a downstream gene, fluctuations in the input are likely to be transmitted, resulting in well-coordinated outputs. Therefore, our simulations represent a conservative scenario for coordination. Regulators that control diverse suites of downstream genes will see benefits from coordination of multiple types of downstream genes. Overall, we found that dynamic and noise-driven coordination can play a bet-hedging role when multiple genes or stress-response mechanisms need to be coordinated without adding to the overall cost.

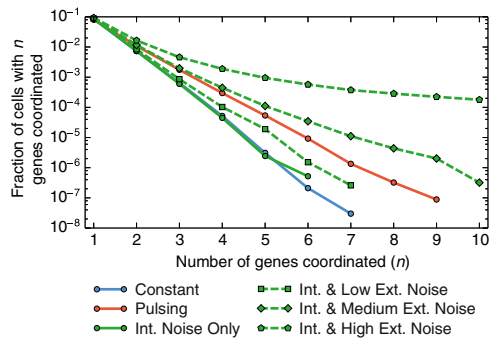

FIGURE 4 Fraction of cells with all downstream genes coordinated as a function of the number of downstream genes, *n*. The benefits of coordination from fluctuating input dynamics are more pronounced as the number of downstream genes increases. Note that in all cases, input dynamics provide higher levels of coordination than does a constant input. Increases in extrinsic noise increase coordination. Conditions show a different maximum number of coordinated genes because not all input cases are sufficient to ensure coordination within a set size of simulated population. To see this figure in color, go online.

SUPPORTING MATERIAL

Supporting Materials and Methods, Supporting Results, seven figures, and two tables are available at http://www.biophysj.org/biophysj/supplemental/S0006-3495(14)01233-8.

ACKNOWLEDGMENTS

We thank N. Rossi and T. Tomko for their critical reading of the manuscript. This research was supported by the National Institutes of Health (1R01AI102922) and by start-up funding from the University of Vermont.

REFERENCES

1. Fraser, D., and M. Kaern. 2009. A chance at survival: gene expression noise and phenotypic diversification strategies. *Mol. Microbiol.* 71: 1333–1340.
2. Balaban, N. Q., J. Merrin, …, S. Leibler. 2004. Bacterial persistence as a phenotypic switch. *Science.* 305:1622–1625.
3. Lewis, K. 2010. Persister cells. *Annu. Rev. Microbiol.* 64:357–372.
4. Süel, G. M., J. Garcia-Ojalvo, …, M. B. Elowitz. 2006. An excitable gene regulatory circuit induces transient cellular differentiation. *Nature.* 440:545–550.
5. Süel, G. M., R. P. Kulkarni, …, M. B. Elowitz. 2007. Tunability and noise dependence in differentiation dynamics. *Science.* 315:1716–1719.
6. Keren, I., N. Kaldalu, …, K. Lewis. 2004. Persister cells and tolerance to antimicrobials. *FEMS Microbiol. Lett.* 230:13–18.
7. Newman, J. R. S., S. Ghaemmaghami, …, J. S. Weissman. 2006. Single-cell proteomic analysis of *S. cerevisiae* reveals the architecture of biological noise. *Nature.* 441:840–846.
8. Blake, W. J., G. Balázsi, …, J. J. Collins. 2006. Phenotypic consequences of promoter-mediated transcriptional noise. *Mol. Cell.* 24: 853–865.
9. Arbel-Goren, R., A. Tal, …, J. Stavans. 2013. Effects of post-transcriptional regulation on phenotypic noise in *Escherichia coli*. *Nucleic Acids Res.* 41:4825–4834.
10. Neildez-Nguyen, T. M. A., A. Parisot, …, A. Paldi. 2008. Epigenetic gene expression noise and phenotypic diversification of clonal cell populations. *Differentiation.* 76:33–40.
11. Stewart-Ornstein, J., J. S. Weissman, and H. El-Samad. 2012. Cellular noise regulons underlie fluctuations in *Saccharomyces cerevisiae*. *Mol. Cell.* 45:483–493.
12. Elowitz, M. B., A. J. Levine, …, P. S. Swain. 2002. Stochastic gene expression in a single cell. *Science.* 297:1183–1186.
13. Levine, J. H., Y. Lin, and M. B. Elowitz. 2013. Functional roles of pulsing in genetic circuits. *Science.* 342:1193–1200.
14. Purvis, J. E., and G. Lahav. 2013. Encoding and decoding cellular information through signaling dynamics. *Cell.* 152:945–956.
15. Hao, N., and E. K. O'Shea. 2012. Signal-dependent dynamics of transcription factor translocation controls gene expression. *Nat. Struct. Mol. Biol.* 19:31–39.
16. Hansen, A. S., and E. K. O'Shea. 2013. Promoter decoding of transcription factor dynamics involves a trade-off between noise and control of gene expression. *Mol. Syst. Biol.* 9:704.
17. Cai, L., C. K. Dalal, and M. B. Elowitz. 2008. Frequency-modulated nuclear localization bursts coordinate gene regulation. *Nature.* 455: 485–490.
18. Wakamoto, Y., N. Dhar, …, J. D. McKinney. 2013. Dynamic persistence of antibiotic-stressed mycobacteria. *Science.* 339:91–95.
19. Charlebois, D. A., G. Balázsi, and M. Kærn. 2014. Coherent feedforward transcriptional regulatory motifs enhance drug resistance. *Phys. Rev. E Stat. Nonlin. Soft Matter Phys.* 89:052708.
20. Alon, U. 2007. Network motifs: theory and experimental approaches. *Nat. Rev. Genet.* 8:450–461.
21. Luscombe, N. M., M. M. Babu, …, M. Gerstein. 2004. Genomic analysis of regulatory network dynamics reveals large topological changes. *Nature.* 431:308–312.
22. Locke, J. C. W., J. W. Young, …, M. B. Elowitz. 2011. Stochastic pulse regulation in bacterial stress response. *Science.* 334:366–369.
23. Barbosa, T. M., and S. B. Levy. 2000. Differential expression of over 60 chromosomal genes in *Escherichia coli* by constitutive expression of MarA. *J. Bacteriol.* 182:3467–3474.
24. Martin, R. G., and J. L. Rosner. 2002. Genomics of the marA/soxS/rob regulon of *Escherichia coli*: identification of directly activated promoters by application of molecular genetics and informatics to microarray data. *Mol. Microbiol.* 44:1611–1624.
25. Dadiani, M., D. van Dijk, …, E. Segal. 2013. Two DNA-encoded strategies for increasing expression with opposing effects on promoter dynamics and transcriptional noise. *Genome Res.* 23:966–976.
26. Dunlop, M. J., R. S. Cox, 3rd, …, M. B. Elowitz. 2008. Regulatory activity revealed by dynamic correlations in gene expression noise. *Nat. Genet.* 40:1493–1498.
27. Munsky, B., G. Neuert, and A. van Oudenaarden. 2012. Using gene expression noise to understand gene regulation. *Science.* 336:183–187.
28. Boettiger, A. N. 2013. Analytic approaches to stochastic gene expression in multicellular systems. *Biophys. J.* 105:2629–2640.
29. Raj, A., and A. van Oudenaarden. 2008. Nature, nurture, or chance: stochastic gene expression and its consequences. *Cell.* 135:216–226.
30. Raj, A., C. S. Peskin, …, S. Tyagi. 2006. Stochastic mRNA synthesis in mammalian cells. *PLoS Biol.* 4:e309.
31. Megerle, J. A., G. Fritz, …, J. O. Rädler. 2008. Timing and dynamics of single cell gene expression in the arabinose utilization system. *Biophys. J.* 95:2103–2115.
32. Dekel, E., and U. Alon. 2005. Optimality and evolutionary tuning of the expression level of a protein. *Nature.* 436:588–592.
33. Wood, K. B., and P. Cluzel. 2012. Trade-offs between drug toxicity and benefit in the multi-antibiotic resistance system underlie optimal growth of *E. coli*. *BMC Syst. Biol.* 6:48.
34. Wood, K. B., K. C. Wood, …, P. Cluzel. 2014. Uncovering scaling laws to infer multidrug response of resistant microbes and cancer cells. *Cell Reports.* 6:1073–1084.
35. Gillespie, D. T. 1977. Exact stochastic simulation of coupled chemical-reactions. *J. Phys. Chem. A.* 81:2340–2361.
36. Bliss, C. I. 1939. The toxicity of poisons applied jointly. *Ann. Appl. Biol.* 26:585–615.
37. Greco, W. R., G. Bravo, and J. C. Parsons. 1995. The search for synergy: a critical review from a response surface perspective. *Pharmacol. Rev.* 47:331–385.
38. Garcia-Bernardo, J., and M. J. Dunlop. 2013. Tunable stochastic pulsing in the *Escherichia coli* multiple antibiotic resistance network from interlinked positive and negative feedback loops. *PLOS Comput. Biol.* 9:e1003229.
39. Martin, R. G., E. S. Bartlett, …, M. E. Wall. 2008. Activation of the *Escherichia coli* marA/soxS/rob regulon in response to transcriptional activator concentration. *J. Mol. Biol.* 380:278–284.
40. Shahrezaei, V., J. F. Ollivier, and P. S. Swain. 2008. Colored extrinsic fluctuations and stochastic gene expression. *Mol. Syst. Biol.* 4:196.
41. Gillespie, D. T. 1996. Exact numerical simulation of the Ornstein-Uhlenbeck process and its integral. *Phys. Rev. E Stat. Phys. Plasmas Fluids Relat. Interdiscip. Topics.* 54:2084–2091.
42. Rosenfeld, N., J. W. Young, …, M. B. Elowitz. 2005. Gene regulation at the single-cell level. *Science.* 307:1962–1965.
43. Fox, R. F., I. R. Gatland, …, G. Vemuri. 1988. Fast, accurate algorithm for numerical simulation of exponentially correlated colored noise. *Phys. Rev. A.* 38:5938–5940.
44. Peccoud, J., and B. Ycart. 1995. Markovian modeling of gene-product synthesis. *Theor. Popul. Biol.* 48:222–234.
45. Larson, D. R. 2011. What do expression dynamics tell us about the mechanism of transcription? *Curr. Opin. Genet. Dev.* 21:591–599.
46. Kaern, M., T. C. Elston, …, J. J. Collins. 2005. Stochasticity in gene expression: from theories to phenotypes. *Nat. Rev. Genet.* 6:451–464.
47. Lee, P., B.-R. Cho, …, J.-S. Hahn. 2008. Yeast Yak1 kinase, a bridge between PKA and stress-responsive transcription factors, Hsf1 and Msn2/Msn4. *Mol. Microbiol.* 70:882–895.

48. Sakurai, H., and Y. Enoki. 2010. Novel aspects of heat shock factors: DNA recognition, chromatin modulation and gene expression. *FEBS J.* 277:4140–4149.

49. Tay, S., J. J. Hughey, …, M. W. Covert. 2010. Single-cell NF-kappaB dynamics reveal digital activation and analogue information processing. *Nature.* 466:267–271.

50. Ashall, L., C. A. Horton, …, M. R. H. White. 2009. Pulsatile stimulation determines timing and specificity of NF-kB-dependent transcription. *Science.* 324:242–246.

51. Martin, R. G., and J. L. Rosner. 2004. Transcriptional and translational regulation of the marRAB multiple antibiotic resistance operon in *Escherichia coli*. *Mol. Microbiol.* 53:183–191.

52. Wall, M. E., D. A. Markowitz, …, R. G. Martin. 2009. Model of transcriptional activation by MarA in *Escherichia coli*. *PLOS Comput. Biol.* 5:e1000614.

53. Charlebois, D. A., N. Abdennur, and M. Kaern. 2011. Gene expression noise facilitates adaptation and drug resistance independently of mutation. *Phys. Rev. Lett.* 107:218101.

54. Davidson, C. J., and M. G. Surette. 2008. Individuality in bacteria. *Annu. Rev. Genet.* 42:253–268.

55. Kussell, E., R. Kishony, …, S. Leibler. 2005. Bacterial persistence: a model of survival in changing environments. *Genetics.* 169:1807–1814.